

Formation and structural characterization of nanocrystalline Si/SiC multilayers grown by hot filament assisted chemical vapor deposition using CH₃SiH₃ gas jets

Ikoma, Yoshifumi

Department of Materials Science and Engineering, Kyushu University

Okuyama, Ryouusuke

Department of Materials Science and Engineering, Kyushu University

Arita, Makoto

Department of Materials Science and Engineering, Kyushu University

Motooka, Teruaki

Department of Materials Science and Engineering, Kyushu University

<https://hdl.handle.net/2324/26481>

出版情報 : Thin Solid Films. 518 (14), pp.3759-3762, 2010-05-03. Elsevier
バージョン :
権利関係 : (C) 2009 Elsevier B.V.



Formation and structural characterization of nanocrystalline Si/SiC multilayers grown by hot filament assisted chemical vapor deposition using CH_3SiH_3 gas jets

Yoshifumi Ikoma*, Ryousuke Okuyama, Makoto Arita, Teruaki Motooka

Department of Materials Science and Engineering, Kyushu University

744 Motooka, Fukuoka 819-0395, Japan

We report on the formation and the structural characterization of nanocrystalline Si/SiC (*nc*-Si/SiC) multilayers on Si(100) by hot-filament assisted chemical vapor deposition using CH_3SiH_3 gas pulse jets. Si rich amorphous SiC ($a\text{-Si}_{1-x}\text{C}_x$, $x \sim 0.33$) was initially grown at the substrate temperature (T_s) of 600 °C with heating a hot filament at ~2000 °C. The following crystalline SiC layers were grown at $T_s = 850$ °C without utilizing a hot filament. When the $a\text{-Si}_{1-x}\text{C}_x$ layer was ultrathin (<2 nm) on Si(100), this $a\text{-Si}_{1-x}\text{C}_x$ layer was transformed to a single epitaxial SiC layer during the subsequent SiC growth process. The Si{111} faceted pits were formed at the SiC/Si(100) interface due to Si diffusion processes from the substrate. When the thickness of the initial $a\text{-Si}_{1-x}\text{C}_x$ layer was increased to ~5 nm, a double layer structure was formed in which this amorphous layer was changed to *nc*-Si and *nc*-SiC was grown on the top resulting in the considerable reduction of the {111} faceted pits. It was found that *nc*-SiC was formed by consuming the Si atoms uniformly diffused from the $a\text{-Si}_{1-x}\text{C}_x$ layer below and that Si nanocrystals were generated in the $a\text{-Si}_{1-x}\text{C}_x$ layers due to the annealing effect during further multilayer growths.

Keywords: Chemical vapor deposition; Si; SiC; multilayer; Nanocrystal; Cross-sectional transmission electron microscopy; X-ray photoelectron spectroscopy

* Corresponding author. Tel.: +81-92-802-2966, Fax.: +81-92-802-2990

E-mail address: ikoma@zaiko.kyushu-u.ac.jp

1. Introduction

Semiconductor multilayer structures have been widely investigated for applications to high-performance quantum electronic [1] and optoelectronic [2] devices. Especially, Si-based multilayers are important due to the compatibility of the existing Si device technologies. Si-based multilayer structures have been studied by using various material systems such as Si/Si_{1-x}Ge_x [3], hydrogenated amorphous Si (*a*-Si:H)/*a*-Si_{1-x}N_x:H [4], and *a*-Si/SiO₂ [5, 6].

SiC is a wide band gap semiconductor and is a suitable material for high-speed and high-power electronic devices [7]. Since the Si/SiC heterostructure has relatively large valence and conduction band offsets [8], it may be promising to fabricate Si-based quantum devices. In case of crystalline SiC, cubic 3C-SiC has a band gap of 2.2 eV and is the only polytype which can be epitaxially grown on Si substrates in spite of a large (20%) lattice mismatch. Although many studies have been reported for the growth of 3C-SiC on Si substrate [9], little work has been done for the crystalline 3C-SiC/Si multilayer structures [10,11]. In case of utilizing amorphous SiC (*a*-Si_{1-x}C_x), the band gap can be flexibly controlled by changing the C concentration x [12]. Recently, magnetron sputtering is widely utilized for growing *a*-Si(:H)/*a*-SiC(:H) [13] and *a*-Si_{1-x}C_x/SiC [14] multilayers.

One of the alternative methods to form Si/SiC multilayers is chemical vapor deposition (CVD). Especially, pulse jet CVD is a promising method for ultrathin film growths [15,16]. Previously, we reported the formation of Si/SiC/Si(100) structure and showed that epitaxial Si layers were formed on epitaxially grown thin (~3 nm) SiC films on Si(100) by exposure of Si₃H₈ pulse jets [17]. When the number of Si₃H₈ jet pulses was reduced, crystalline Si dots were found to grow on the epitaxial SiC film [18,19]. We also reported that Si/SiC heterostructures can be realized by using single gas source CH₃SiH₃ pulse jet CVD with a hot filament [20,21]. However, continuous two-dimensional Si/SiC multilayers were not observed when the thickness of the Si layer was decreased to ~100 nm. Besides, {111} faceted pits were introduced at the SiC/Si(100) interface due to the diffusion of Si atoms

outward from the substrate [17,20]. In this study, we investigated the formation and the structural characterization of nanocrystalline Si/SiC (*nc*-Si/SiC) multilayers on Si(100) formed by alternating growths of *a*-Si_{1-x}C_x and SiC layers utilizing hot filament assisted CVD of CH₃SiH₃ gas pulse jets.

2. Experimental procedure

The CVD chamber was equipped with mechanical and turbomolecular pumps and had a base pressure of $\sim 10^{-6}$ Pa. The details are described elsewhere [21]. The Si(100) substrates were cleaned by the conventional RCA method [22]. The substrates were introduced into the chamber after being dipped in aqueous 5% buffered HF in order to remove surface oxides. Electronic grade CH₃SiH₃ was introduced into the growth chamber using a Parker Hannifin Corporation Series 9 pulse valve with a nozzle diameter of 0.8 mm. The distance between the nozzle and the Si substrate was approximately 20 cm. The pulse width and frequency were set at 120 μ s and 10 Hz, respectively. A tungsten hot filament was placed in front of the Si substrate. The distance between the filament and the substrate was ~ 2 cm. The substrate and the hot filament temperatures were measured by a W/Re thermocouple and a pyrometer, respectively. During *a*-Si_{1-x}C_x growths, the substrate and the hot filament temperatures were set at 600 °C and ~ 2000 °C, respectively. In case of SiC growths, the hot filament was turned off and the substrate temperature was increased to 850 °C. Cross-sectional transmission electron microscopy (XTEM) observations were carried out using JEOL Ltd. JEM 200CX and JEM 2000EX operated at 200 kV, and JEM 4000EX at 400 kV. X-ray photoelectron spectroscopy (XPS) measurements were performed in a Perkin–Elmer Corporation PHI 5600 ESCA system using Mg K α x-ray source. The depth profiles of the chemical shifts were examined using Ar⁺ sputtering at 3 kV.

3. Results and discussion

In order to confirm the *a*-Si_{1-x}C_x growth by CH₃SiH₃ jets using a hot filament, we

carried out the film growth on Si(100) and characterized the film by XTEM and XPS. Fig. 1 shows the XTEM bright-field image and diffraction pattern obtained from the sample grown by CH_3SiH_3 jet exposures of 18000 pulses. The bright-field image shows that the film with the thickness of 10 nm is uniformly grown on Si(100). The diffraction spots corresponding to Si(100) substrate and a weak amorphous halo pattern can be seen in the diffraction pattern. Fig. 2 shows the XPS spectra of Si 2p, C 1s, and O 1s for various sputtering time obtained from the same sample of Fig. 1. Other elements such as tungsten were lower than the XPS detection limit. The sample surface is composed of oxidized Si judged by the peak positions of Si 2p ~ 104 eV and O 1s ~ 533 eV as well as the carbon contamination C 1s ~ 286 eV which indicates the existence of C–O bonds. The peaks at ~ 100 eV in Si 2p and ~ 283 eV in C 1s indicate that Si–C bonds exist in the film. After sputtering for 1 min, the peaks which are related to surface oxide and carbon contaminants disappear and a broad peak at ~ 100 eV in Si 2p and a peak at ~ 283 eV in C 1s become strong. In addition, a weak peak at ~ 532 eV exists in O 1s. These peaks suggest that Si–Si, Si–C, and Si–O bonds exist in the film. The atomic percentages of Si, C, and O which are estimated from each peak area and atomic sensitivity factor in this region are 72%, 24% and 4%, respectively. These results indicate that the obtained film is Si rich $a\text{-Si}_{1-x}\text{C}_x$ ($x \sim 0.33$). The inclusion of O atoms in the film may be due to the incorporation of outgases from the chamber wall and the hot filament during the film growth.

In order to form multilayer structures, we repeated the $a\text{-Si}_{1-x}\text{C}_x$ and SiC growths with various pulse conditions. We firstly formed an ultrathin (< 2 nm) $a\text{-Si}_{1-x}\text{C}_x$ layer by 3000 pulses of CH_3SiH_3 jet exposure with heating a hot filament and then grew the SiC film by 3000 pulses of CH_3SiH_3 jet exposure. It is found that a single layer with the thickness of ~ 5 nm is formed on the substrate surface shown in the XTEM bright-field image of Fig. 3. The diffraction pattern shows that the $a\text{-Si}_{1-x}\text{C}_x$ layer is transformed to an epitaxial SiC layer during the subsequent SiC growth process. The existence of $\{111\}$ faceted pits in the XTEM image of Fig. 3 indicates that both the $a\text{-Si}_{1-x}\text{C}_x$ layer and the substrate act as additional

sources of Si atoms during the SiC growth.

Fig. 4 shows the XTEM bright-field image and diffraction pattern obtained from the sample which was repeated four times of $a\text{-Si}_{1-x}\text{C}_x$ and SiC growths. During this multilayer formation, we increased the numbers of CH_3SiH_3 pulse jet exposure to 9000 and 6000 pulses for $a\text{-Si}_{1-x}\text{C}_x$ and SiC growths, respectively. The bright-field image shows the multilayer which consists of 8 layers. The light and dark contrast regions correspond to $a\text{-Si}_{1-x}\text{C}_x$ and SiC layers, respectively. It should be noted that the thickness of the $a\text{-Si}_{1-x}\text{C}_x$ layers decreases to ~ 3 nm while the estimated thickness of the $a\text{-Si}_{1-x}\text{C}_x$ layer from the bright-field image of Fig. 1 is 5 nm. This thickness decrease after the SiC growth has been also observed in case of Si layers because the SiC growth is sustained by not only CH_3SiH_3 molecules but also additional Si atoms diffused from the Si layer below [20]. In the present case, it can be explained that each SiC layer is grown by uniformly consuming the Si atoms from the $a\text{-Si}_{1-x}\text{C}_x$ layer below. Also, it is found that the SiC growth rate decreases and the thickness is ~ 6 nm although the number of the CH_3SiH_3 pulses is increased to 6000. This growth-rate decrease suggests that SiC densely nucleates on the $a\text{-Si}_{1-x}\text{C}_x$ layer, resulting in the suppression of Si atoms diffused outward from the $a\text{-Si}_{1-x}\text{C}_x$ layer below [23]. A weak ring pattern corresponding to SiC together with a weak halo probably due to $a\text{-Si}$ in the diffraction pattern indicates that the multilayer is mainly composed of $nc\text{-SiC}$ and $a\text{-Si}_{1-x}\text{C}_x$.

Figs. 5(a)~5(c) show the XTEM bright-field, dark-field images, and diffraction pattern, respectively, obtained from the sample which was repeated the growths of $a\text{-Si}_{1-x}\text{C}_x$ and SiC layers for 10 times. The numbers of the CH_3SiH_3 pulse jet exposures were set at 9000 and 3000 for $a\text{-Si}_{1-x}\text{C}_x$ and SiC growths, respectively. The multilayer structure which is composed of 20 layers is observed in Fig. 5(a). The thickness of each layer is ~ 5 nm. The discontinuous regions of the multilayer structures exist near the substrate surface. The dark-field image of Fig. 5(b) shows that these discontinuous regions are composed of crystalline Si. In the diffraction pattern of Fig. 5(c), the ring patterns of Si and SiC in addition to a weak halo indicate that the multilayer is mainly composed of $nc\text{-Si}$ and $nc\text{-SiC}$. The

high-resolution TEM image of Fig. 6 shows that there exist large and small lattice images which correspond to Si and SiC, respectively. The typical size of both *nc*-Si and *nc*-SiC is ~5 nm. The interfaces of adjacent layers are not atomically flat due to relatively large roughness of 2 ~ 3 nm.

The formation of *nc*-Si has been also observed in postdeposition annealing of *a*-Si_{1-x}C_x films prepared using magnetron sputtering by Song *et al.* [24] They also reported the *a*-Si_{1-x}C_x/SiC multilayer formation by alternating deposition of *a*-Si_{0.96}C_{0.04} and near-stoichiometric SiC layers and observed that the interfaces of adjacent layers became rough after annealing at ≥900 °C [14]. In our multilayer formation utilizing single gas source CH₃SiH₃ pulse jet CVD, since the sample was repeatedly heated at 850 °C during the SiC layer growths, Si nanocrystals were likely generated from the *a*-Si_{1-x}C_x layers by the simultaneous annealing. The generation of *nc*-Si from *a*-Si_{1-x}C_x layers was not clear at the initial stage of the multilayer formation shown in Fig. 4, but it became remarkable in the 10-layer sample as shown in the diffraction pattern of Fig. 5(c). Especially, the observation of discontinuous regions near the substrate surface shown in Figs. 5(a) and 5(b) indicates that the Si nano-crystallization was enhanced by further multilayer growths. The generation of *nc*-SiC as well as *nc*-Si from *a*-Si_{1-x}C_x layers may also induce the rough interfaces of adjacent layers in the multilayer shown in Fig. 6. It should be noted that the thickness decrease of the *a*-Si_{1-x}C_x layers after the SiC growths affected the crystallinity of the following SiC layers in the present experimental conditions. In case of the *a*-Si_{1-x}C_x layer grown on the Si substrate by CH₃SiH₃ jets at 3000, this ultrathin (<2 nm) *a*-Si_{1-x}C_x layer was completely consumed by subsequent 3000 pulses of CH₃SiH₃ jet exposure and a single epitaxial SiC layer was consequently grown on the Si substrate as shown in Fig. 3. When the number of the CH₃SiH₃ pulses was increased to 9000 and formed thick (~5 nm) *a*-Si_{1-x}C_x layers, these *a*-Si_{1-x}C_x layers still remained after SiC growths as shown in Figs. 4 and 5. SiC random nucleation may well occur on these *a*-Si_{1-x}C_x layers resulting in the formation of *nc*-SiC.

4. Conclusion

We investigated the formation and the structural characterization of *nc*-Si/SiC multilayers on Si(100) by hot-filament assisted CVD using CH₃SiH₃ gas pulse jets. When the *a*-Si_{1-x}C_x ($x \sim 0.33$) layer was ultrathin (<2 nm) on Si(100), this *a*-Si_{1-x}C_x layer was transformed to an epitaxial SiC layer during the subsequent SiC growth process. When the thickness of the initial *a*-Si_{1-x}C_x layer was increased to ~5 nm, the {111} faceted pits were considerably reduced and the *nc*-Si/SiC multilayers were formed by repeating the *a*-Si_{1-x}C_x and SiC growths. It was found that *nc*-SiC was formed by consuming the Si atoms uniformly diffused from the *a*-Si_{1-x}C_x layer below, and that Si nanocrystals were generated in the *a*-Si_{1-x}C_x layers due to the annealing effect during further multilayer growths.

Acknowledgement

This work was supported by the Global COE Program ‘Science for Future Molecular Systems’ from the Ministry of Education, Culture, Sports, Science and Technology of Japan.

References

1. R. Tsu, L. Esaki, Appl. Phys. Lett. 22 (1973) 562.
2. B. F. Levine, J. Appl. Phys. 74 (1993) R1.
3. Y. Shiraki, A. Sakai, Surf. Sci. Rep. 59 (2005) 153.
4. B. Abeles, T. Tiedje, Phys. Rev. Lett. 51 (1983) 2003.
5. Z. H. Lu, D. J. Lockwood, J.-M. Baribeau, Nature 378 (1995) 258.
6. D. J. Lockwood, Z. H. Lu, J.-M. Baribeau, Phys. Rev. Lett. 76 (1996) 539.
7. R. F. Davis, G. Kelner, M. Shur, J. W. Palmour, J. A. Edmond, Proc. IEEE 79 (1991) 677.
8. U. Baumann, J. Pezoldt, V. Cimalla, O. Nennwitz, F. Schwier, D. Schipanski, in: S. Nakashima, H. Matsunami, S. Yoshida, H. Harima (Eds.), 6th International Conference on Silicon Carbide and Related Materials 1995, Kyoto, Japan, September 18-21, 1995, Institute of Physics Conference Series 142 (1996) 149.
9. H. Matsunami, Diamond Related Mater. 2 (1993) 1043.
10. Q. Wahab, L. Hultman, I. P. Ivanov, M. Willander, J.-E. Sundgren, J. Mater. Res. 10 (1995) 139.
11. L.-O. Björketun, L. Hultman, O. Kordina, J.-E. Sundgren, J. Mater. Res. 13 (1998) 2632.
12. J. Bullot, M. P. Schmidt, Phys. Stat. Sol., B 143 (1987) 345.
13. Y. Suzaki, T. Shikama, H. Kakiuchi, A. Takeuchi, K. Yoshii, H. Kawabe, J. Magn. Magn. Mater. 126 (1993) 22.
14. D. Song, E.-C. Cho, G. Conibeer, Y. Huang, C. Flynn, M. A. Green, J. Appl. Phys. 103 (2008) 083544.
15. T. Motooka, H. Abe, P. Fons, T. Tokuyama, Appl. Phys. Lett. 63 (1993) 3473.
16. Y. Ikoma, T. Endo, F. Watanabe, T. Motooka, Jpn. J. Appl. Phys., Part 2, 38 (1999) L301.
17. Y. Ikoma, T. Endo, F. Watanabe, T. Motooka, Appl. Phys. Lett. 75 (1999) 3977.
18. Y. Ikoma, T. Tada, K. Uchiyama, F. Watanabe, T. Motooka, Solid State Phenom. 78/79 (2001) 157.
19. Y. Ikoma, R. Ohtani, N. Matsui, T. Motooka, J. Vac. Sci. Technol., B 21 (2003) 2492.

20. Y. Ikoma, R. Ohtani, T. Motooka, Mater. Sci. Forum 457-460 (2004) 325.
21. R. Ohtani, Y. Ikoma, T. Motooka, Jpn. J. Appl. Phys. 45 (2006) 2514.
22. W. Kern, D. A. Puotinen, RCA Rev. 31 (1970) 187.
23. J. P. Li, A. J. Steckl, J. Electrochem. Soc. 142 (1995) 634.
24. D. Song, E.-C. Cho, Y.-H. Cho, G. Conibeer, Y. Huang, S. Huang, M. A. Green, Thin Solid Films 516 (2008) 3824.

List of figure captions

Fig 1. XTEM bright-field image and diffraction pattern obtained from the sample grown by CH_3SiH_3 jet exposures of 18000 pulses. The spot pattern indicates crystalline Si due to the crystal Si substrate. A weak halo coexists in the diffraction pattern. The thickness of the film is 10 nm.

Fig 2. XPS spectra of Si 2p, C 1s, and O 1s obtained from $a\text{-Si}_{1-x}\text{C}_x/\text{Si}(100)$ after Ar^+ sputtering for (a) 0 min, (b) 1 min, and (c) 10 min. The spectra (c) are the same as those from the Si substrate.

Fig 3. XTEM bright-field image and diffraction pattern obtained from the sample grown by 3000 pulses of CH_3SiH_3 jet exposure with a hot filament heating, and 3000 pulses of CH_3SiH_3 jet exposure without hot filament assistance. The SiC film is epitaxially grown on Si(100).

Fig 4. XTEM bright-field image and diffraction pattern obtained from the sample which was repeated four times of $a\text{-Si}_{1-x}\text{C}_x$ and SiC growths. The numbers of CH_3SiH_3 pulse jets were set at 9000 and 6000 for $a\text{-Si}_{1-x}\text{C}_x$ and SiC growths, respectively.

Fig 5. (a) XTEM bright-field image, (b) bright-field image, and (c) diffraction pattern of the sample which was repeated 10 times of $a\text{-Si}_{1-x}\text{C}_x$ and SiC growths. The numbers of CH_3SiH_3 pulse jets were set at 9000 and 3000 for $a\text{-Si}_{1-x}\text{C}_x$ and SiC growths, respectively.

Fig 6. High-resolution TEM image of $nc\text{-Si}/\text{SiC}$ multilayers which is the same sample of Fig. 5. This image was taken near from the interface between the multilayer and Si(100) substrate.

Fig 1

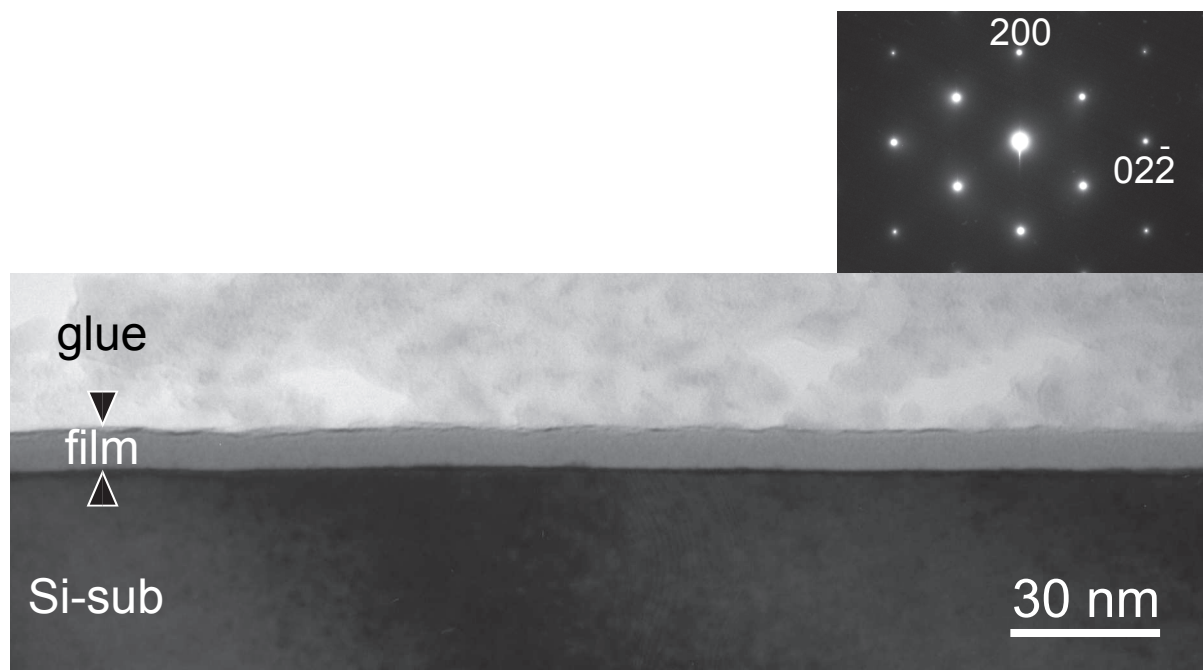


Fig 2

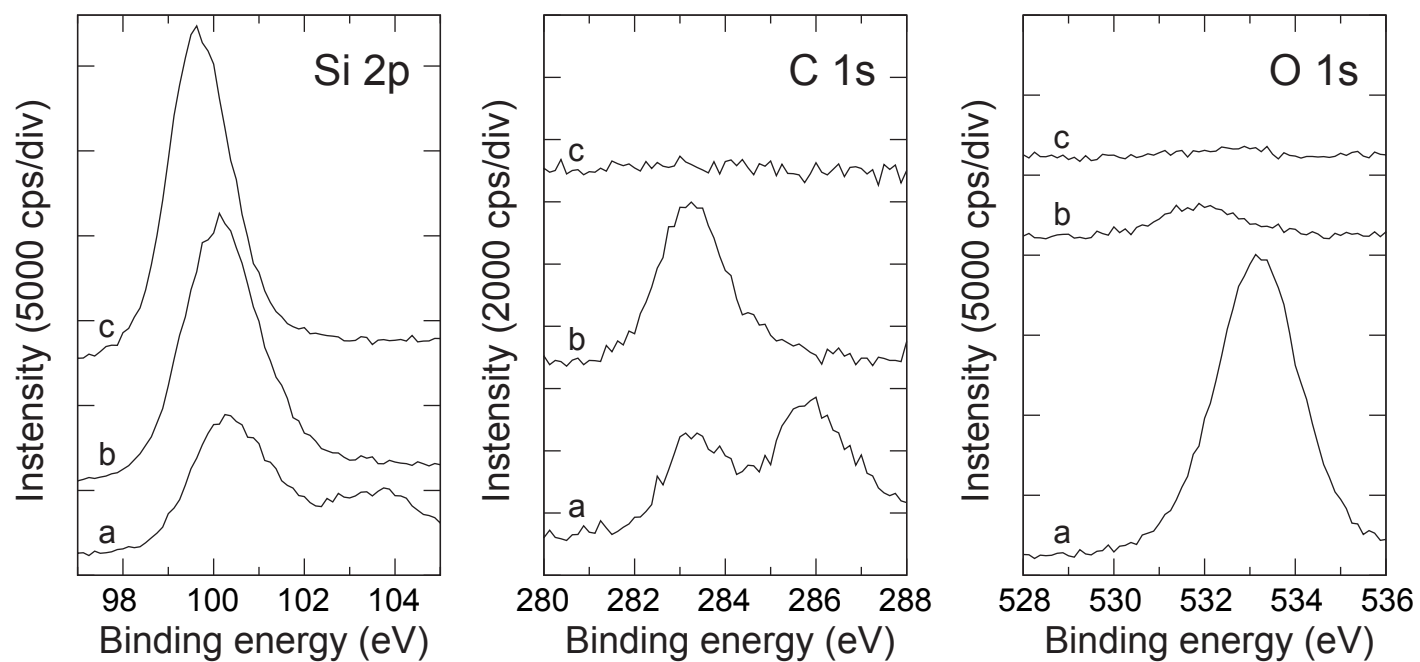


Fig 3

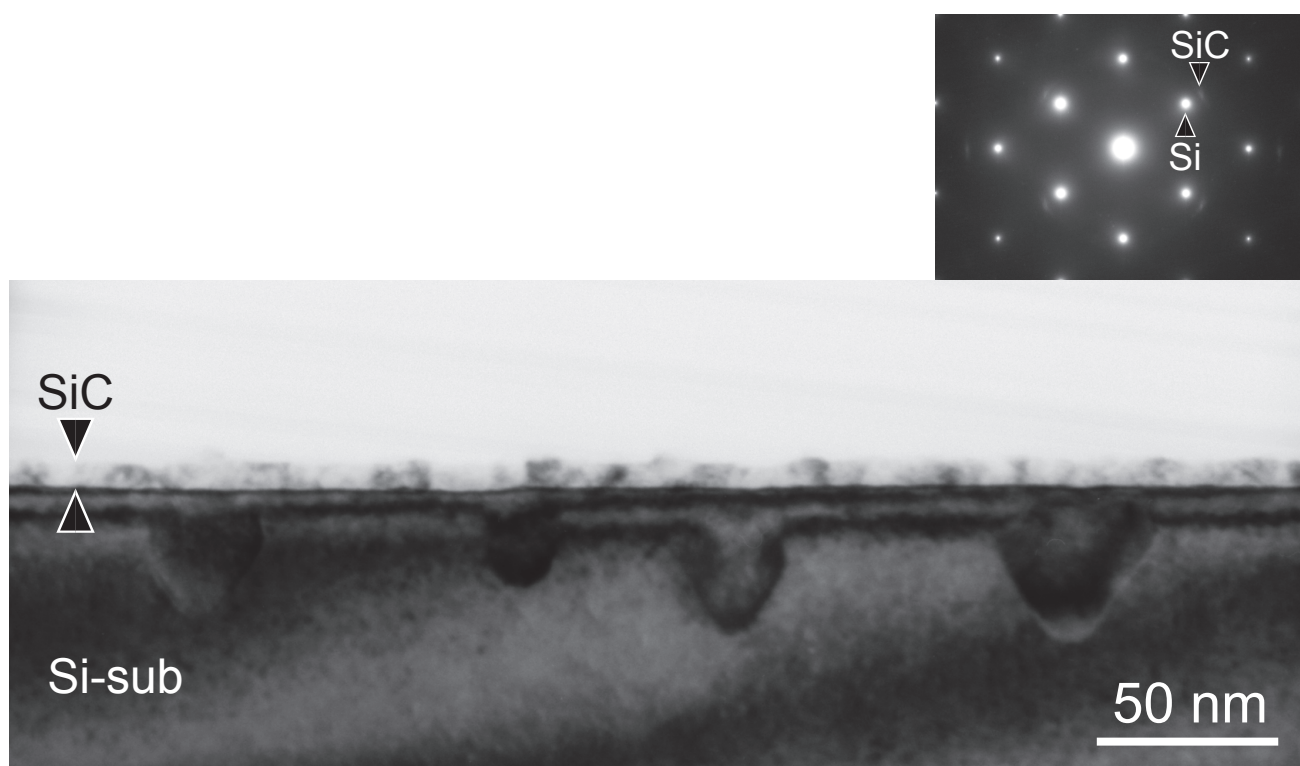


Fig 4

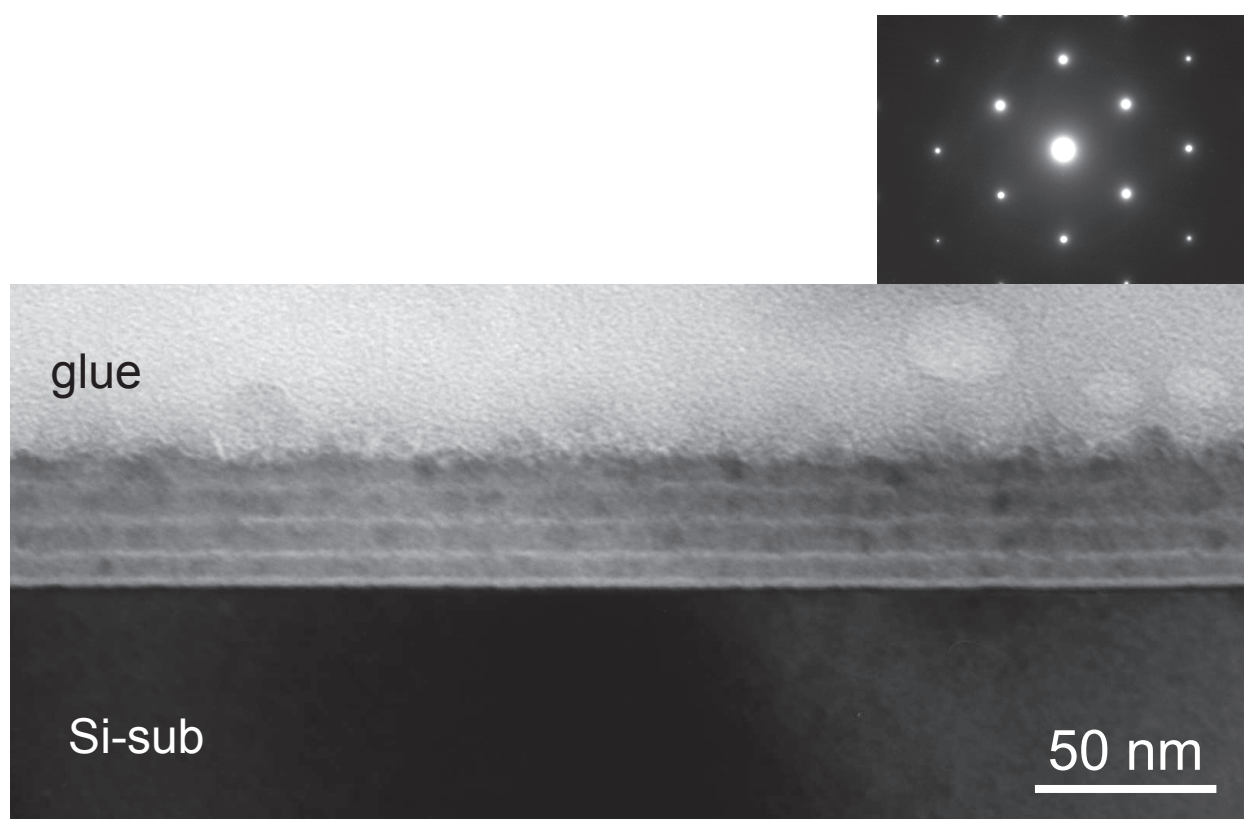


Fig 5

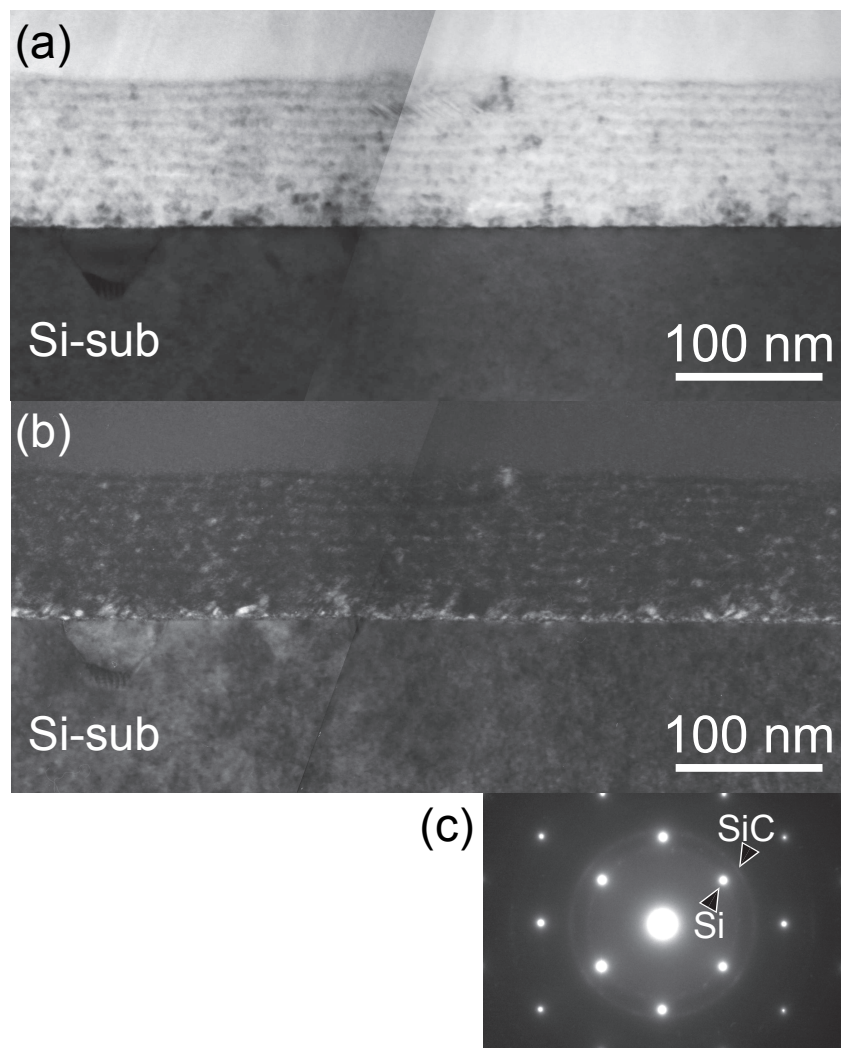


Fig 6

